Materials Science and Engineering C 33 (2013) 4504–4511

Contents lists available at ScienceDirect

Materials Science and Engineering C

journal homepage: www.elsevier.com/locate/msec

Modified insulator semiconductor electrode with functionalized nanoparticles for *Proteus mirabilis* bacteria biosensor development

Yosra Braham [a,*], Houcine Barhoumi [a], Abderrazak Maaref [a], Amina Bakhrouf [b], Nicole Jaffrezic-Renault [c,**]

[a] Laboratoire des interfaces, et des matériaux avancés, Faculté des sciences de Monastir, 5019, Tunisia
[b] Laboratoire d'analyse, de traitement et de valorisation des polluants de l'environnement et des produits, Faculté de pharmacie, Monastir 5000, Tunisia
[c] Laboratoire de Sciences Analytiques, UMR CNRS 5280, Université Claude Bernard-Lyon1, 69622 Villeurbanne Cedex, France

ARTICLE INFO

Article history:
Received 9 October 2012
Received in revised form 29 March 2013
Accepted 19 June 2013
Available online 28 June 2013

Keywords:
Proteus mirabilis
Fe_3O_4
PAH and PSS polyelectrolytes
Kinetic parameters capacity–potential measurements C(V)
Insulator semiconductor IS
Bacterial adhesion

ABSTRACT

The development of enzymatic sensors for biological purposes such as biomedicine, pharmacy, food industry, and environmental toxicity requires the purification step of the enzyme. To prevent the loss of the enzyme activity, a new strategy is held in order to immobilize the bacteria. It will constitute the biological sensing element leading to a high operational stability and multiple adaptations to various conditions such as temperature, pH and ionic strength changes. In this work we describe the development of a urea biosensor by immobilizing *Proteus mirabilis* bacteria onto an insulator–semiconductor electrode on functionalized Fe_3O_4 nanoparticles (NPs), using cationic, Poly (allylamine hydrochloride) then anionic, Poly (sodium 4-styrenesulfonate) polyelectrolytes, BSA (serum bovin albumin), and glutaraldehyde as a cross-linking agent. The response of *P. mirabilis* to urea addition is evaluated in homogeneous and heterogeneous phases. Before the immobilization step, the activity of urease produced from the *P. mirabilis* bacteria was attempted using the ion ammonium selective electrodes (ISEs). Adhesion of the bacteria cells on IS electrodes have been studied using contact angle measurements. After immobilization of the bacteria, on the ($Si/SiO_2/Si_3N_4$) and (Si/SiO_2) substrates, the relationship between the evolution of the flat band potential ΔV_{FB} and the urea concentration is found to be linear for values ranging from 10^{-2} M to 10^{-5} M.

1. Introduction

Various applications in physics, biology, chemistry, and electronics involve the development of efficient, simple, stable, and low cost sensors. In this context, biosensors based on semiconductor structures, especially the ion-sensitive field-effect transistors (ISFETs) as transducers and the microorganisms as bio-receptor, offer innovative solution. The ISFET has several advantages, such as small size, rapid response, low output impedance and low cost by mass-device production. Different substrates are widely used in sensor devices, such as silicon nitride, for its low permeability and structural porosity but also silicon dioxide, or silica despite its high permeability toward water and other impurities [1,2].

Due to their desirable chemical–physical, electronic, and optical properties, metal nanoparticles have attracted much attention and demonstrated a wide range of applications. The use of nanoparticles is one of the most interesting approaches to improve the performances of biosensor [3–5]. The Fe_3O_4 nanoparticles have been for instance considered as suitable for immobilization of enzyme due to their super paramagnetic behavior and low toxicity [6,7].

The determination of urea in body fluids is of great interest in biomedical analyses. Since this gives indication of a potential renal dysfunction. A variety of biosensors based on urease have been developed for the selective determination of urea. The detection principle is based on the enzymatic reaction catalyzed by urease according to the following equation:

$$CO(NH_2)_2 + 3H_2O \xrightarrow{\text{Urease}} CO_2 + 2NH_4^+ + 2OH^- \quad (1)$$

A variety of enzymes are found in bacteria like *Proteus mirabilis* [8], fungi, higher plants, and in soil as a soil enzyme [9]. Bacteria cells accordingly offer a multitude of choice for the development of new biosensors with low cost and naturally optimized [10].

Our study was carried out on Electrolyte–Insulator–Semiconductor (EIS) structures with silicon dioxide and silicon nitride insulators, functionalized with Fe_3O_4 NPs, used for the biosensor elaboration based on Enterobacteriaceae *P. mirabilis*. The electronic devices (IS) are developed to measure pH, through the capacitive technique. The response of biosensor using electrochemical methods is studied in terms of detection limits, sensitivity, linear range and activity.

Our findings indicating that the hydrophilic *P. mirabilis* strain adheres better to the hydrophobic IS-coated with PAH, illustrate the

* Corresponding author. Tel.: +216 73 500 276; fax: +216 73 500 278.
** Corresponding author.
E-mail addresses: braham.yosra@yahoo.fr (Y. Braham), nicole.jaffrezic@univ-lyon.fr (N. Jaffrezic-Renault).

0928-4931/$ – see front matter © 2013 Elsevier B.V. All rights reserved.
http://dx.doi.org/10.1016/j.msec.2013.06.031

decrease of the Michaelis constant (K_m) value relative to the high affinity of urease from *P. mirabilis* to urea, and confirm the biocompatibility of the nanoparticles.

2. Experiments

2.1. Reagents

The iron oxide carboxyl-modified magnetic nanoparticles (NPs, diameter = 200 nm, density of carboxyl groups >350 μmolg^{-1}, stored in an aqueous suspension of 0.09% NaN_3) were obtained from Ademtech. PAH (poly (allylamine hydrochloride), and PSS (poly (sodium 4-styrene sulfonate) polyelectrolytes (PEs), bovine serum albumin (BSA), glycerol and glutaraldehyde were purchased from Sigma-Aldrich. Phosphate buffer solution (PBS) was used in this study (7 mM Na_2HPO_4, 3 mM NaH_2PO_4 and 130 mM NaCl at pH 7.4).

P. mirabilis (*P.m*) bacteria were provided by the bacteria department of pharmacy faculty, and diluted in PBS solution at a concentration of 20×10^7 CFU mL^{-1}.

The insulator/semiconductor (IS) structures, Si/SiO_2 and $Si/SiO_2/Si_3N_4$ were purchased from the Institute of Microtechnology, University of Neuchatel (Switzerland). Their surface was 1 cm^2. The studied $Si/SiO_2/Si_3N_4$ structures were based on a p-type silicon substrate, 400 μm thickness, with 10 Ω cm resistivity, covered with 50 nm of thermally grown silicon dioxide and 100 nm of silicon nitride prepared by Low Pressure Chemical Vapor Deposition (LPCVD) technique at 750 °C. Si/SiO_2 structures were based on (100) p-type silicon wafer with a 3–5 Ω cm resistivity and 400 μm thickness. The insulating layer was a thermally grown (53 ± 2 nm) silicon dioxide layer. The ohmic contact on reverse side of the silicon was obtained by deposition of a gold layer under vacuum. The area of the working electrode defined by an O-ring seal was 0.07 cm^2.

2.2. Insulator semiconductor electrode cleaning

The working electrodes were treated using three organic solvents and sulfochromic mixture, in order to obtain absorbent, clean and active insulator semiconductor structures [11]. They were cleaned by ultrasounds using: trichloroethylene, acetone and isopropanol in this order. Then, the surfaces were activated by sulfochromic acid, to generate silanol groups (Si–OH) of silicon oxide [12] (isoelectronic point $pH_i = 2$) which play the role of active centers (Eq. (2)).

$$\begin{aligned} &SiOH + H^+ \xrightarrow{pH<pH_i=2} SiOH_2^+ \\ &SiOH \xrightarrow{pH>pH_i=2} SiO^- + H^+ \end{aligned} \quad (2)$$

In the case of silicon nitride, characterized by an isoelectronic point $pH_i = 4$, the reactivity of surface was determined by the presence of $Si–NH_2$ et Si–OH sites. In contact with water, the latter give rise to the following equilibriums [13,14] (Eq. (3)–(5)).

$$SiOH + H^+ \xrightarrow{pH<pH_i=4} SiOH_2^+ \quad (3)$$

$$SiNH_2 + H^+ \xrightarrow{pH<pH_i=4} SiNH_3^+ \quad (4)$$

$$SiOH \xrightarrow{pH>pH_i=4} SiO^- + H^+ \quad (5)$$

2.3. Electrochemical characterization and instrumentation

2.3.1. Potentiometric measurements based on ion selective electrode (ISE)

Potentiometric method based on ion-selective electrodes (ISEs) offers advantages such as simple procedure, relatively fast response time, non-destructive analysis, wide linear range with moderate selectivity [15–19], extensively applied for determination of ion concentration.

In this work we used potentiometric instrument for direct measurement of ammonium ion concentration in solution, in order to detect *P. mirabilis* urease activity. This was achieved using ammonium selective PVC membrane ISEs, with Ag/AgCl reference electrode.

2.3.2. Capacity–potential measurements based on insulator–semiconductor (IS) electrodes

Capacitance method was based on the measurement of the local pH change of the electrolyte near the (IS) which originates from the enzymatic reaction of urea hydrolyzed by urease from *P. mirabilis* according to Eq. (1). The C (V) measurement results were treated using the standard series model to rise to the capacitance curves, from which the flat band potential shift (ΔV) was determined. The variation of ΔV_{FB} obeys Nernst's law [19–22], and the response of the sensor was defined as the slope of the curve ΔV_{FB} as a function of the ionic potential (-logarithm of the concentration) [23]. Then we can determine the detection limits, the sensitivity and the linear range of our biosensor.

In this study, we illustrated the capacitive biosensor [24–26], prepared by the immobilization of *P. mirabilis* bacteria. Experiments were performed in an electrochemical cell with three electrodes, comprising the modified insulator semiconductor electrode (0.07 cm^2) as a working electrode, a platinum plate (0.45 cm^2) as an auxiliary electrode and a saturated calomel electrode (SCE) as a reference, connected to a potentiostat–galvanostat (VOLTALAB-40 PGZ/301). The amplitude of the alternative signal was 10 mV at 10 kHz frequency. All the experiments were made in a dark Faraday cage at room temperature.

2.4. Contact angle measurements

The contact angle is an important parameter in surface science. It is a common measure of the hydrophobicity of a solid surface [27]. It is generally agreed that the physicochemical properties of bacterial cells and substrate surfaces are the main factors mediating bacterial adhesion [28–30]. It is assumed that bacterial cells and substrate hydrophobicity are the key parameters controlling the non-specific interactions of the adhesion process [31]. Contact angle measurements with three different liquids (water, formamide and diiodomethane) were performed with model contact angle instrument "Digidrop" from the GBX society (Romans, France). Every reported contact angle measurements represented an average value of at least three separated drops on different areas of the given wafer. The size and volume of the drops were kept constant [32].

Wettability, hydropholicity and contact angle of the bacteria membrane were evaluated. Furthermore, surface energy components, the total energy (γ_s), the dispersive energy (γ^{LW}), the acid base energy ($\gamma^{AB} = 2\sqrt{\gamma^+ \cdot \gamma^-}$), the acid energy ($\gamma^+$) and the basic energy ($\gamma^-$) were determined from the wetting angle (Θ) according to the Van Oss equation with polar and apolar liquids [33].

2.5. Preparation of the P. mirabilis bacteria biosensors

To acquire a high sensitivity and a good repetition biosensor, various working conditions were examined. These include the presence of BSA, glycerol, the nanoparticle concentration (0.01 mg mL^{-1} in 500 μL of PBS) [26], the bacteria concentration (20×10^7 CFU mL^{-1}), the cross-linking time (30 min), the buffer solution concentration PBS (10 mM), the number of the polyelectrolyte layers (n = 3) [24].

The bacteria mixture was prepared by dissolving 5 mg of BSA in 100 μL PBS bacteria solution, containing 10 μL glycerol at pH 7.4.

The initial NPs suspension (1/500) was sonicated for 15 min, then coated during 20 min, with an initial "preconditioning" layer of PAH (5 mg L^{-1}) which provides a positive charge, followed by a layer of PSS (5 mg L^{-1}) of opposite charge to form the first PE bilayer (n = 1). The NPs were further coated sequentially with PEs, in the alternating order PAH/PSS until three bilayers, followed by a layer of PAH.

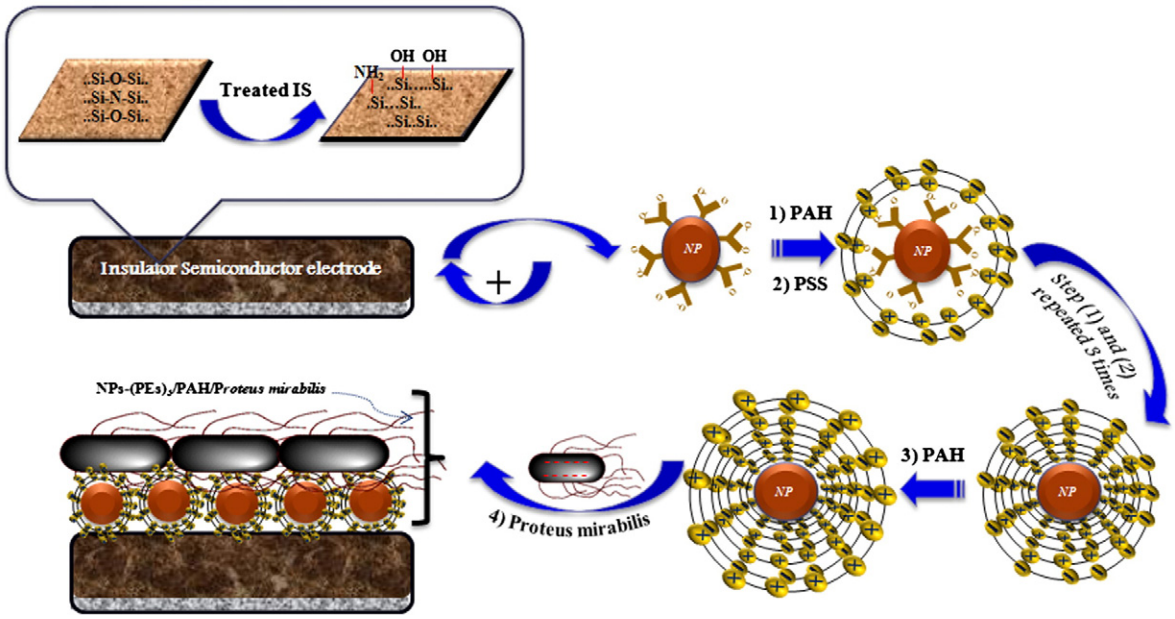

Fig. 1. Schematic capacitive urea biosensor using Fe_3O_4 and polyelectrolytes.

We obtained (NPs-(PAH-PSS)$_n$/PAH) with n spanning from 1 to 3. The PE rich supernatant phase was then eliminated and the NPs were rinsed twice in ultrapure water [25].

Then we deposited 10 µL of (NPs-(PAH-PSS)$_3$/PAH) on IS cleaned electrode, followed by 10 µL of bacteria mixture. Finally, the IS/NPs-(PAH/PSS)$_3$/PAH/bacteria biosensor, (Fig. 1) was kept in glutaraldehyde vapor for 30 min to allow the reticulation of bacteria.

3. Results and discussion

3.1. The enzymatic kinetics in homogeneous phase

3.1.1. Study of the urea concentration effect

Urea interaction with *P. mirabilis* was monitored in bacterial solution (12 mL) by measuring produced ammonium ion (Eq. (1)). Fig. 2 shows an increase of ammonium ion concentration with the increase of urea injected and illustrates the kinetic behavior of the enzymatic reaction according to the concentration of the urea in solution. Urea penetrates in bacterial cells via transport system and complex with urease in the cytoplasmic membrane. This attests the permeability of *P. mirabilis* membrane to urea.

According to Fig. 2, the curve corresponding to urea concentration 7.69 mM enables us to determine the activity of urease from *P. mirabilis*. This kinetic obeys the Michaelis law and shows that the response increases with time, until reaching a plateau for ammonium ion concentrations higher or equal to 0.0869 M, corresponding to the saturation of urease active sites by urea molecules. We can conclude that the enzymatic activity of urease in solution is equal to 20 µmol min^{-1} $(40 \times 10^7\ CFU)^{-1}$.

3.1.2. Determination of kinetic parameters

To evaluate the catalytic activity of free bacteria, we determined the kinetic parameters like the affinity (k_m) and the maximum speed of catalysis (V_{max}). In reality the Michaelis constant (k_m) is a very useful fundamental characteristic of the enzyme–substrate couple. The equation of Michaelis–Menten (Eq. (6)) allows calculating the speed of reaction:

$$V = \frac{V_{max}[urea]}{k_m + [urea]} \tag{6}$$

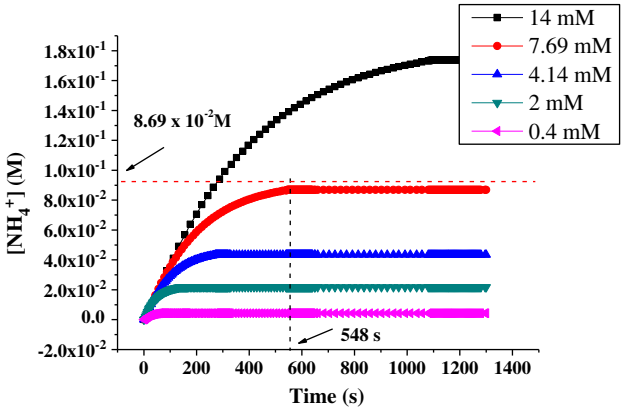

Fig. 2. Kinetic behavior of the enzymatic reaction according to the urea concentration in homogeneous phase.

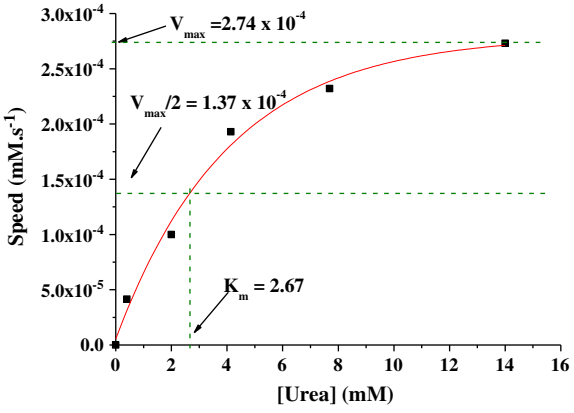

Fig. 3. Michaelis–Menten kinetics according to free *Proteus mirabilis*.

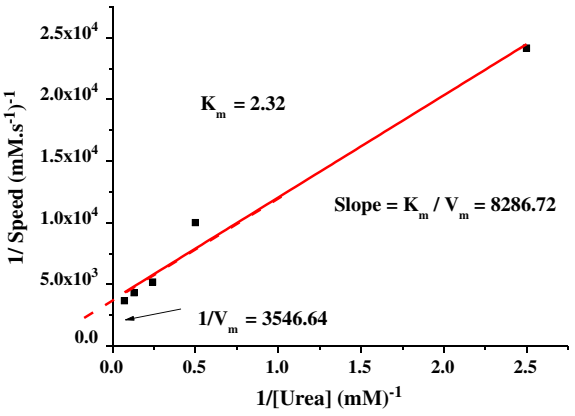

Fig. 4. Graphic representation of Lineweaver–Burk for free *Proteus mirabilis*.

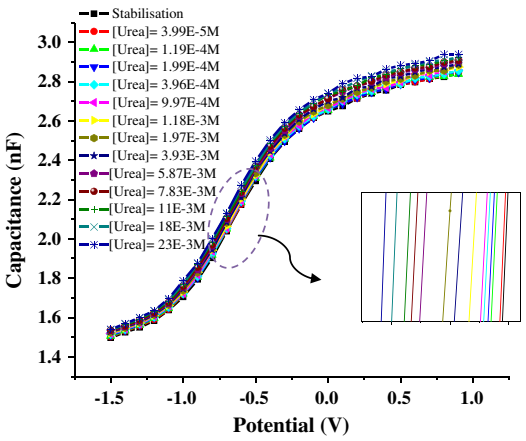

Fig. 6. Capacitance spectra of the $Si/SiO_2/Si_3N_4/P.m$ biosensor for different urea concentrations performed in 10 mM PBS buffer solution.

The determination of initial speed is done by measuring the product concentration according to time; it corresponds to the slope of the tangent at the origin. That enables us to plot the Michaelis–Menten curve: $[NH_4^+] = f(t)$ with $V_i = f[urea]$, (Fig. 3). This curve presents a plateau for urea concentrations higher or equal to 14 mM, corresponding to the saturation of the enzyme active sites by urea molecules. A speed V_{max} equal to 16.4 mM min^{-1} and K_m equal to 2.67 mM are found with a correlation coefficient R^2 equal to 0.96.

For more accurate measurements, the Hans Lineweaver and Dean Burk method was used (Fig. 4). It was proposed following a linearization of Michaelis–Menten (Eq. (7)).

$$\frac{1}{V} = \frac{k_m}{V_{max}} \frac{1}{[urea]} + \frac{1}{V_{max}} \tag{7}$$

This method gives $V_{max} = 16$ mM min^{-1}, $k_m/V_{max} = 8286.72$ and $k_m = 2.32$ mM. This last value is close to the value obtained with free urease found in the literature [24], comprised between 1 and 5 mM. This can be explained by the high specificity of the urease enzyme from *P. mirabilis* for its substrate.

3.2. The enzymatic kinetics in heterogeneous phase

Before evaluating the behavior of immobilized *P. mirabilis* in the presence of urea, the pH sensitivity of the bare Si/SiO_2 and $Si/SiO_2/Si_3N_4$ has been proven. The C (V) results (Fig. 5) of a pH-sensitive bare IS structure in the concentration range from pH 3 to pH 10 show that the pH response is linear with an average sensitivity of 32 and 50 ± 2 mV/pH, which is in good agreement with the pH-sensitivity values reported in the literature for the SiO_2 and Si_3N_4 layer [34,35].

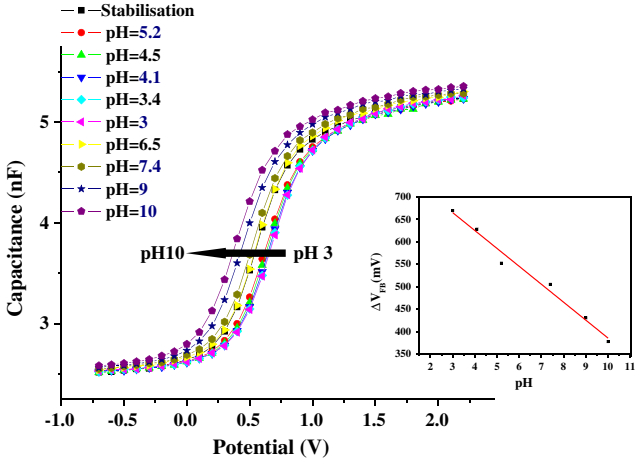

Fig. 5. Typical set of C (V) curves of a pH-sensitive Si/SiO_2 structure. The inset shows the corresponding calibration curve. Measuring conditions: PBS buffer solutions in the pH range between pH 3 and pH l0.

3.2.1. Study of the urea concentration effect

The analytical performance of the bacteria biosensors was evaluated in PBS solution for different urea concentrations from 3.99×10^{-2} mM to 23 mM via the electrochemical C (V) method. The recorded sensor output signal correlates directly with the respective urea concentration in the solution and the amplitude of the alternative signal was 10 mV at 10 kHz frequency. As shown in Fig. 6, the concentration of OH ions derived from the enzymatic reaction increases with increasing the urea concentration. As a consequence the spectrum capacity-potential shifts to the negative flat band potential.

The electrochemical response of $Si/SiO_2/Si_3N_4/P.m$ biosensor was given by the shift of the flat band potential as function of the urea concentration (Fig. 7).

As a result, sensitivity equal to 40 mV/pH was observed. The lower sensitivity of the functionalized IS structure could be due to the adhesion of bacteria which dominates the surface of the IS electrode. So the effect of the flat band potential becomes less sensitive to the

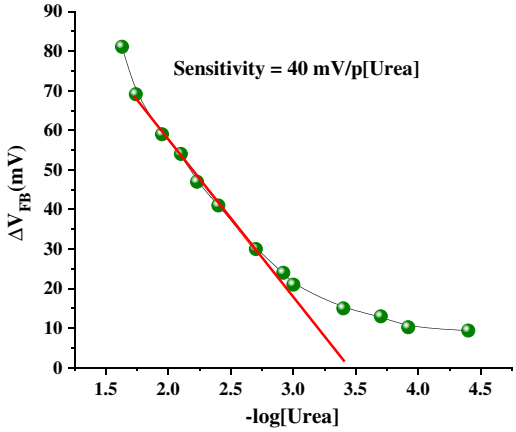

Fig. 7. Variation of the flat band potential of $Si/SiO_2/Si_3N_4/P.m$ biosensor for different urea concentrations performed in 10 mM PBS buffer solution.

Table 1
Elaboration of *Proteus mirabilis* biosensor.

Biosensors	Sensitivity (mV/p[Urea])	Linear range (mM)	Detection limit (mM)
$Si/SiO_2/P.m$	37	[3.94; 23]	1.99×10^{-1}
$Si/SiO_2/PAH/P.m$	67	[4; 18]	8.5×10^{-1}
$Si/SiO_2/PAH/P.m$ + BSA + glycerol + glutaraldehyde	123	[7.9; 18]	2.23
$Si/SiO_2/NPs\text{-}(PAH/PSS)_3/PAH/P.m$ + BSA + glycerol + glutaraldehyde	**163**	**[15.6; 23.2]**	**8.31×10^{-1}**
$Si/SiO_2/Si_3N_4/P.m$	40	[1.99; 18]	18
$Si/SiO_2/Si_3N_4/PAH/P.m$	45	[1; 11]	5×10^{-1}
$Si/SiO_2/Si_3N_4/PAH/P.m$ + BSA + glycerol + glutaraldehyde	51	[15; 23]	2.63×10^{-1}
$Si/SiO_2/Si_3N_4/NPs\text{-}(PAH/PSS)_3/PAH/P.m$ + BSA + glycerol + glutaraldehyde	**84**	**[11; 23]**	**4.67×10^{-1}**

pH local variation since bacteria mask the active sites of the Si_3N_4 substrate.

To obtain the optimum electrochemical features of the fabricated biosensor, various biosensors were testing. The average urea sensitivity for four tested biosensors (IS/*P.m*; IS/PAH/*P.m*; IS/PAH/*P.m* + BSA + glycerol + glutaraldehyde; IS/NPs-$(PAH/PSS)_3$/PAH/*P.m* + BSA + glycerol + glutaraldehyde), from each insulator semiconductor electrode was about 37, 67, 123 and 163 mV/pUrea for the silicon dioxide sensors, and 40, 45, 51 and 84 mV/pUrea for silicon nitride, respectively (Table 1).

Compared to these biosensors, the greatest sensitivity to urea has been obtained for the IS functionalized with an electrostatic binding between the polyelectrolyte multilayer $(PAH/PSS)_3$/PAH and the Fe_3O_4 nanoparticles. The good performance of the IS/NPs-$(PAH/PSS)_3$/PAH/*P.m* structure results from the large surface of contact between bacteria and the surrounding medium. This vast specific zone is at the origin of the particular properties of nanoparticles which give a strong reactivity to the immobilized bacteria surface.

In comparison with the IS/NPs-$(PAH/PSS)_3$/PAH/*P.m* + BSA + glycerol + glutaraldehyde systems, we observe a noticeable decrease in the sensitivity of others biosensors, IS/PM; IS/PAH/*P.m* and IS/PAH/*P.m* + BSA + glycerol + glutaraldehyde.

These results confirm the positive role played by the nanoparticles in the elaboration procedure, leading to a very stable detection and a high sensitive urea biosensor equal to 163 for silicon dioxide (Fig. 8) and 84 mV/pUrea for silicon nitride (Fig. 9).

The behavior of the urea biosensor was studied with or without the presence of BSA, glycerol and glutaraldehyde (Tables 1–2). The sensitivity is higher for the biosensor treated by BSA, glutaraldehyde and glycerol, which allow a better adhesion, reticulation and more regular distribution of bacteria without destroying the mechanical properties of the deposit membrane.

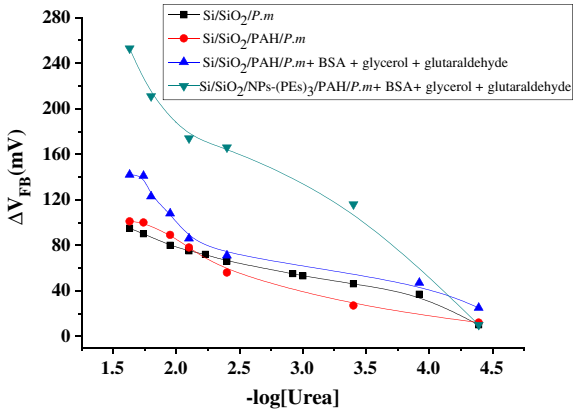

Fig. 8. Variation of the flat band potential of $Si/SiO_2/P.m$ biosensors for different urea concentrations performed in 10 mM PBS buffer solution.

3.2.2. Determination of kinetic parameters

In this study we have determined the kinetic behavior of immobilized *P. mirabilis* bacteria in the presence of the Fe_3O_4 nanoparticles. As shown in Figs. 10 and 11, the determined K_m value using the Michaelis–Menten graphic and the Lineweaver–Burk representations was about 0.9 mM for the silicon dioxide sensors and silicon nitride, with a correlation coefficient R^2 equal to 0.99 (Table 2).

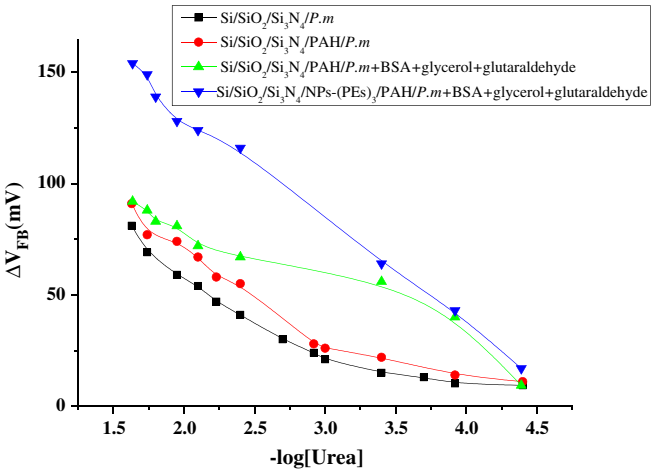

Fig. 9. Variation of the flat band potential of $Si/SiO_2/Si_3N_4/P.m$ biosensors for different urea concentrations performed in 10 mM PBS buffer solution.

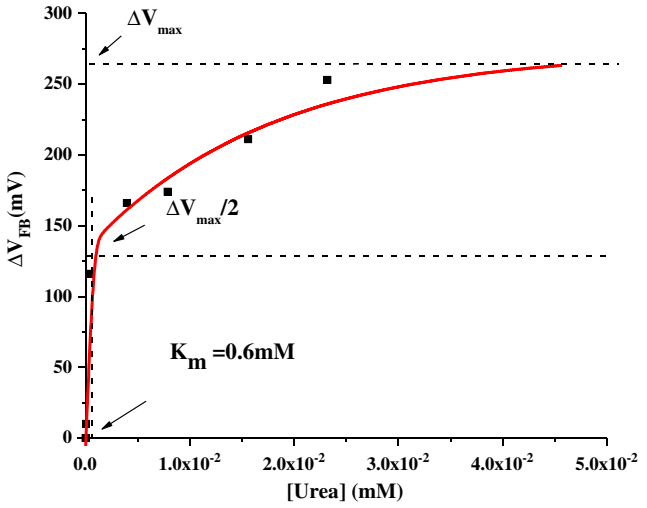

Fig. 10. Michaelis–Menten kinetics according to immobilized *Proteus mirabilis*.

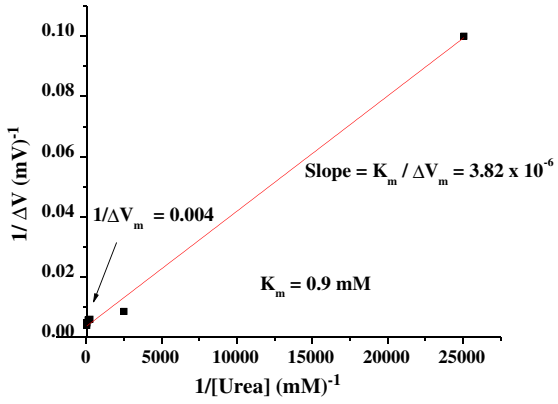

Fig. 11. Graphic representation of Lineweaver–Burk corresponding to immobilized *Proteus mirabilis*.

Table 2
Kinetic parameters of urease from *Proteus mirabilis* immobilized obtained from Michaelis–Menten and Lineweaver–Burk methods.

Biosensors	Sensitivity (mV/p[Urea])	K_m (mM)
Si/SiO_2/*P.m*	37	1
Si/SiO_2/PAH/*P.m*	67	4
Si/SiO_2/PAH/*P.m* + BSA + glycerol + glutaraldehyde	123	6.3
Si/SiO_2/NPs-$(PAH/PSS)_3$/PAH/*P.m* + BSA + glycerol + glutaraldehyde	**163**	**0.6–0.9**
$Si/SiO_2/Si_3N_4$/*P.m*	40	3.8
$Si/SiO_2/Si_3N_4$/PAH/*P.m*	45	2.4
$Si/SiO_2/Si_3N_4$/PAH/*P.m* + BSA + glycerol + glutaraldehyde	51	1.6
$Si/SiO_2/Si_3N_4$/NPs-$(PAH/PSS)_3$/PAH/*P.m* + BSA + glycerol + glutaraldehyde	**84**	**0.4–0.9**

This result is close to that obtained for the free urease (1 mM < K_m < 5 mM). In addition, the found K_m value explains the high affinity of *P. mirabilis* urease for its substrate and confirms the biocompatibility of the nanoparticles used without any inhibitory effect.

3.2.3. Contact angle measurements and adhesion tests

In order to check the effectiveness of the functionalization process, contact angle measurements, obtained with water as test liquid (Fig. 12), have been carried out for the bacteria membrane deposited on IS electrodes. The wetting properties have been compared before and after functionalization process.

The values of the contact angles with the different probe liquids and surface energy components for the substrate surfaces and membrane deposed are summarized in Table 3.

The contact angle measurements show that the IS surface is hydrophobic while the bacteria is hydrophilic. It is noted that the electron-donor component of the IS is much higher than the electron-acceptor component, which means that the IS is negatively charged. Also, it can be seen that the SiO_2 is more electron-donating than the Si_3N_4 surface.

We notice an increase in the basic energy (γ^-) of the surface following deposing the bacteria. Indeed, surface becomes richer in groups hydroxid (OH) and carboxyl (RCOOH) coming from the *P. mirabilis* bacteria and nanoparticles [36].

Table 4 presents the contact angles with the different probe liquids for *P. mirabilis* suspended in PBS and then deposited on cellulose acetate membrane filters. With an angle of 18.1° we conclude that the bacterial cell is hydrophilic. The contribution of the electrostatic forces to adhesion is important, since together bacteria and substrate surfaces have generally negative surface potentials, giving rise to repulsive electrostatic interactions (Fig. 12). But the use of polyelectrolyte PAH makes the adhesion possible due to the positive charge of NH_3^+.

Using the thermodynamic approach of the Lifshitz van der Waals (LW) and acid/base (AB) interactions, the total adhesion energy ΔG_{adh}^{Total} of a bacterium (B) to a substrate surface (S) in a suspending liquid (L)

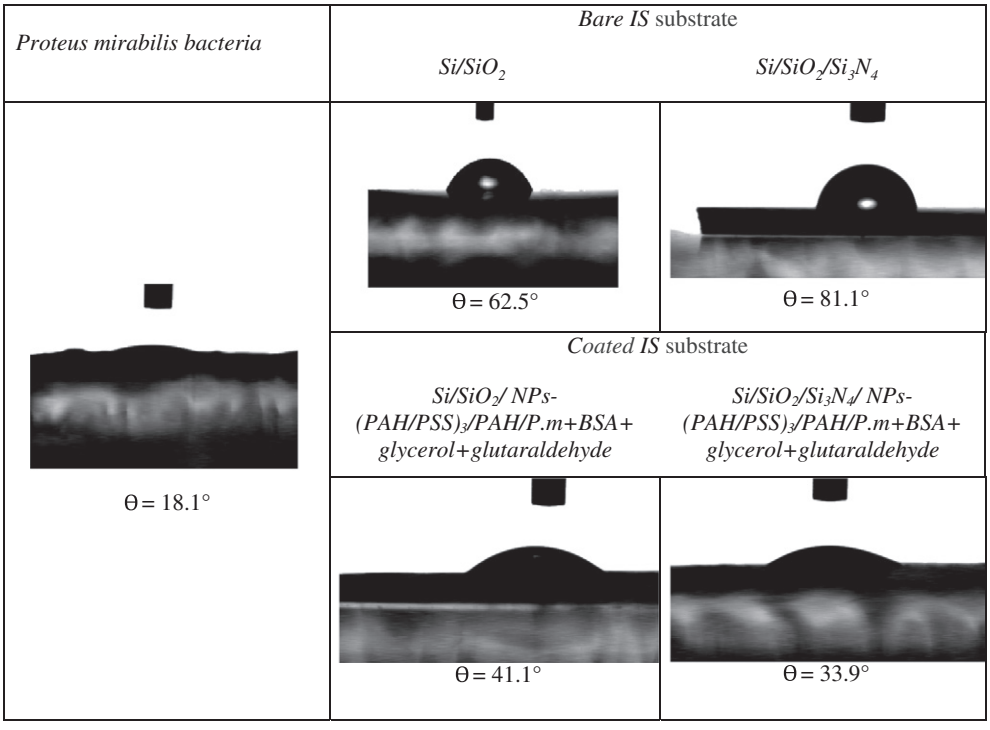

Fig. 12. Schematic representations of contact angles with water for different surface and *Proteus mirabilis*.

Table 3
Contact angles and surface energy components of IS structures.

[a] Contact angle (°)				Surface energy components (mJ m^{-2})				
Materials	Water	Formamide	Diiodomethane	γ^{LW}	γ^{AB}	γ^{+}	γ^{-}	γ^{Total}
Si/SiO_2	62.5	41.0	43.2	38.0	8.1	1.1	14.2	46.0
Si/SiO_2/PAH	78.1	37.0	38.1	40.0	9.0	8.0	3.0	42.0
Si/SiO_2/PAH/*P.m*	26.8	36	36	41.6	1.9	0.0	57.1	43.5
Si/SiO_2/PAH/*P.m* + BSA + glycerol + glutaraldehyde	35.8	26.4	30.5	44	8.1	0.4	39.4	52.2
Si/SiO_2/NPs-$(PAH/PSS)_3$/PAH/*P.m* + BSA + glycerol + glutaraldehyde	41.4	49.8	40.3	39.5	5.4	0.1	51.6	44.9
$Si/SiO_2/Si_3N_4$	81.1	62.6	43.7	35.8	0.9	0.0	6.9	36.6
$Si/SiO_2/Si_3N_4$/PAH	93.1	43.2	43.0	40.1	9.0	8.2	3.1	41.1
$Si/SiO_2/Si_3N_4$/PAH/*P.m*	18.1	34.3	39.8	39.7	6.1	0.1	73.7	45.8
$Si/SiO_2/Si_3N_4$/PAH/*P.m* + BSA + glycerol + glutaraldehyde	33.6	43.0	37.5	40.8	2.3	0.0	55.6	43.1
$Si/SiO_2/Si_3N_4$/NPs-$(PAH/PSS)_3$/PAH/*P.m* + BSA + glycerol + glutaraldehyde	33.9	47.2	41.7	38.7	4.5	0.1	59.7	43.2

[a] The contact angle error is ±3°.

Table 4
Contact angle *measurements* of *Proteus mirabilis* suspended in PBS.

[a] Contact angle (°)				Surface energy components ($mJ.m^{-2}$)				
Bacteria	Water	Formamide	Diiodomethane	γ^{LW}	γ^{AB}	γ^{+}	γ^{-}	γ^{Total}
Proteus mirabilis	18.1	20.2	41.8	37.6	15.8	1.3	55.6	53.5
PBS[b]	–	–	–	22	35.2	17.6	17.6	57.2

[a] The contact angle error is ±3°.
[b] The values of γ^{LW} and γ^{AB} are taken from published data [37].

can be calculated as the sum of the LW component ΔG^{LW}_{adh} and the AB component ΔG^{AB}_{adh} [37–39].

$$\Delta G^{Total}_{adh} = \Delta G^{LW}_{adh} + \Delta G^{AB}_{adh} \quad (8)$$

$$\Delta G^{LW}_{adh} = \left(\sqrt{\gamma^{LW}_B} - \sqrt{\gamma^{LW}_S}\right)^2 - \left(\sqrt{\gamma^{LW}_B} - \sqrt{\gamma^{LW}_L}\right)^2 - \left(\sqrt{\gamma^{LW}_S} - \sqrt{\gamma^{LW}_L}\right)^2 \quad (9)$$

$$\Delta G^{AB}_{adh} = 2\left[\sqrt{\gamma^{+}_L}\left(\sqrt{\gamma^{-}_B} + \sqrt{\gamma^{-}_S} - \sqrt{\gamma^{-}_L}\right) + \sqrt{\gamma^{-}_L}\left(\sqrt{\gamma^{+}_B} + \sqrt{\gamma^{+}_S} - \sqrt{\gamma^{+}_L}\right) - \sqrt{\gamma^{-}_B\gamma^{+}_S} - \sqrt{\gamma^{+}_B\gamma^{-}_S}\right] \quad (10)$$

The prediction of the thermodynamic approach states that adhesion may occur if ΔG^{Total}_{adh} is negative and it is energetically unfavorable if ΔG^{Total}_{adh} is positive.

Using (Eq. (8)–(10)), the values of the interfacial free energy of adhesion of *P. mirabilis* to IS electrodes and its components (LW and AB) are calculated and presented in Table 5. According to the thermodynamic approach, the adhesion is favorable due to negative value of the energy (Table 5). The adhesion process is governed by interactions, the negative value of the LW component adhesion energy indicates that adhesion is favorable onto both substrate functionalized with PAH and nanoparticles coated with $(PAH/PSS)_3$/PAH. This is confirmed by adhesion tests, throughout the total adhesion energy value

Table 5
Lifshitz van der Waals (ΔG^{LW}_{adh}), acid/base (ΔG^{AB}_{adh}) and total (ΔG^{Total}_{adh}) interfacial free energy of adhesion of *Proteus mirabilis* stain on IS surfaces (in millijoules per square meter).

Bacteria	Materials	ΔG^{LW}_{adh}	ΔG^{AB}_{adh}	ΔG^{Total}_{adh} ($mJ\ m^{-2}$)
Proteus mirabilis	Si/SiO_2	−4.25	17.91	13.66
	Si/SiO_2/PAH	−4.71	−6.13	−10.84
	$Si/SiO_2/Si_3N_4$	−3.72	17.78	14.04
	$Si/SiO_2/Si_3N_4$/PAH	−4.73	−6.18	−10.91

(−10.84 and −10.91 mJ m^{-2}). It indicates that *P. mirabilis* strain adheres strongly to the hydrophobic IS surfaces.

4. Conclusion

This work describes an electrochemical biosensor for urea detection using *P. mirabilis* bacteria. The employ of the bacteria containing enzyme as well as the magnetic nanoparticles (Fe_3O_4) can improve the biosensor stability, activity, sensitivity and affinity. The effect of the hydrophobicity on the adhesion of the hydrophilic *P. mirabilis* strain to the hydrophobic IS-coated surfaces was investigated and the adhesion free energy of bacteria to the tested materials based on the thermodynamic approach was evaluated.

The fundamental matters that should be addressed on the implantation in vivo of biofuel cells and the development of new analytical methods, to enable the possibility of immediate and discriminative supervising of some contaminants in a multicomponent sample and then the conversion of the biosensing systems to devices suitable for large scale environmental and food applications.

References

[1] T.L. Chu, J.R. Szedon, C.H. Lee, Solid State Electron. 10 (1967) 897.
[2] H. Barhoumi, A. Maaref, R. Mlika, C. Martelet, N. Jaffrezic-Renault, L. Ponsonnet, Mater. Sci. Eng. C 25 (2005) 61–66.
[3] P.V. Kamat, Photophysical, photochemical and photocatalytic aspects of metal nanoparticles, J. Phys. Chem. B 106 (2002) 7729–7744.
[4] R.J. Gehr, R.W. Boyd, Optical properties of nanostructured optical materials, Chem. Mater. 8 (1996) 1807–1819.
[5] M. Ghaedi, M. Nejati Biyareh, S. Nasiri Kokhdan, S. Shamsaldini, R. Sahraei, A. Daneshfar, S. Shahriyar, Mater. Sci. Eng. C 32 (2012) 725–734.
[6] A.K. Gupta, M. Gupta, Biomaterials 26 (2005) 3995–4021.
[7] F.Y. Cheng, C.H. Su, Y.S. Yang, C.S. Yeh, C.Y. Tsai, C.L. Wu, M.T. Wu, D.B. Shi, Biomaterials 26 (2005) 729–738.
[8] G.M. Ederer, J.H. Chu, D.J. Blazevic, Microbiology 21 (1971) 545.
[9] H.L.T. Mobley, R.P. Hausinger, Microbiol. Rev. 53 (1989) 85–108.
[10] F. Bettaieb et al. (2007), M. Castellarnau et al. (2007), M. Castellarnau et al. (2008), T. Maskow et al. (2006), PCJ. Roach et al. (2003).
[11] H. Barhoumi, A. Maaref, N. Jaffrezic-Renault, Langmuir 26 (2010) 7165.
[12] A. Van den Berg, P. Bergveld, D. Reinhoudt, E. Sudholter, Sensors Actuators 8 (1985) 129.
[13] C. Fung, P. Cheung, W. Ko, IEEE Trans. Electron Devices 33 (1986) 3.
[14] D. Harame, L. Bousse, J. Shott, J. Meindl, IEEE Trans. Electron Devices 34 (1987) 1700.
[15] M. Ghaedi, M. Montazerozohori, A. Mousavi, S. Khodadoust, M. Mansouri, Mater. Sci. Eng. C 32 (2012) 523–529.
[16] M.K. Amini, M. Ghaedi, A. Rafi, I. Mohammad poor-Baltork, K. Niknam, Sens. Actuators B 96 (2003) 669.
[17] M.K. Amini, M. Ghaedi, A. Rafi, M.H. Habbibi, M.M. Zohory, Microchem. J. 75 (2003) 143.
[18] M.K. Amini, M. Ghaedi, A. Rafi, M.H. Habibi, M.M. Zohory, Sensors 3 (2003) 509.
[19] M. Ghaedi, S. Naderi, M. Montazerozohori, R. Sahraei, A. Daneshfar, N. Taghavimoghadam, Mater. Sci. Eng. C 32 (2012) 2274–2279.
[20] F. Aouni, A. Rouis, H. Ben Ouada, R. Mlika, C. Dridi, R. Lamartine, Mater. Sci. Eng. C 24 (2004) 491.
[21] F. Aouni, R. Mlika, C. Martelet, H. Ben Ouada, N. Jaffrezic-Renault, A.P. Soldatkin, Electroanalysis 16 (2004) 1907.
[22] L. Bousse, P. Bergveld, On the impedance of silicon dioxide/electrolyte interface, Electroanal. Chem. 152 (1993) 25–39.

[23] J.L. Diot, J. Joseph, J.R. Martin, P. Clechet, Electroanal. Chem. 75 (1985) 193.
[24] M. Souiri, L. Mora-Ponsonnet, K. Glinel, A. Othmane, T. Jouenne, A.C. Duncan, Surface assembly on biofunctional magnetic nanobeads for the study of protein–ligand interactions, Colloids Surf. B Biointerfaces 68 (2009) 125–129.
[25] S. Ciurli, S. Mangani, Nickel-containing enzymes, in: I. Bertini, A. Sigel, H. Sigel (Eds.), Handbook on Metalloproteins, Marcel Dekker, New York, 2001, p. 669.
[26] Y. Sahraoui, H. Barhoumi, A. Maaref, N. Jaffrezic-Renauld, A novel capacitive biosensor for urea assay based on modified magnetic nanobeads, Sens. Lett. 9 (2011) 1–6.
[27] C.N.C. Lam, R. Wu, D. Li, M.L. Hair, A.W. Neumann, Study of the advancing and receding contact angles: liquid sorption as a cause of contact angle hysteresis, Adv. Colloid Interface Sci. 96 (2002) 169–191.
[28] M.N. Bellon-Fontaine, N. Mozes, H.C. van der Mei, J. Sjollema, O. Cerf, P.G. Rouxhet, H.J. Busscher, A comparison of thermodynamic approaches to predict the adhesion of dairy microorganisms to solid substrata, Cell Biophys. 17 (1990) 93–106.
[29] A.M. Gallardo Moreno, M.L. Gonzalez Martin, C. Perez Giraldo, E. Garduno, J.M. Bruque, A.C. Gomez Garcia, Appl. Environ. Microbiol. 68 (2002) 5784.
[30] J. Wang, N. Huang, C.J. Pan, S.C.H. Kwok, P. Yang, Y.X. Leng, J.Y. Chen, H. Sun, G.J. Wan, Z.Y. Liu, P.K. Chu, Bacterial repellence from polyethylene terephthalate surface modified by acetylene plasma immersion ion implantation-deposition, Surf. Coat. Technol. 186 (2004) 299–304.
[31] S. Bayoudh, A. Othmane, F. Bettaieb, A. Bakhrouf, H. Ben Ouada, L. Ponsonnet, Quantification of the adhesion free energy between bacteria and hydrophobic and hydrophilic substrata, Mater. Sci. Eng. C 26 (2006) 300–305.
[32] A. Marmur, Thermodynamic aspects of contact angle hysteresis, Adv. Colloid Interface Sci. 50 (1994) 121–141.
[33] C.J. Van Oss, R.J. Good, M.K. Chaudhurg, J. Colloid Interface Sci. 28 (1987) 35.
[34] M. Thust, M.J. Schöning, S. Frohnhoff, R. Arens-Fischer, P. Kordos, H. Lüth, Meas. Sci. Technol. 7 (1996) 26.
[35] M. Thust, M.J. Schiining, J. Vetter, P. Kordos, H. Liith, Anal. Chim. Acta 323 (1996) 115–121.
[36] U. Seydel, B. Lindner, H.W. Wollenweber, E.T. Rietschel, European Journal of Biochemistry, Structural studies of the lipid A components of enterobacterial lipopolysaccharides by laser desorption mass spectrometry. Location of acyl groups at the lipid A backbone, Eur. J. Biochem. 145 (1984) 505–550.
[37] N.J. Hallab, K.J. Bundy, K. O'Connor, R.L. Moses, J.J. Jacobs, Evaluation of metallic and polymeric biomaterial surface energy and surface roughness characteristics for directed cell adhesion, Tissue Eng. 7 (2001) 55–71.
[38] M.N. Bellon Fontaine, N. Mozes, H.C. van der Mei, S.J. Jollema, O. Cerf, P.G. Rouxhet, H.J. Busscher, A comparison of thermodynamic approaches to predict the adhesion of dairy microorganisms to solid substrata, Cell Biophys. 17 (1990) 93–106.
[39] C.J. Van Oss, Hydrophobicity of biosurfaces origin, quantitative determination and interaction energies, Colloids Surf. B 5 (1990) 91–110.